



Title	Effects of internal strain and external pressure on electronic structures and optical transitions of self-assembled In xGa 1-xAs/GaAs quantum dots: An experimental and theoretical study
Author(s)	Wen, Y; Yang, M; Xu, SJ; Qin, L; Shen, ZX
Citation	Journal Of Applied Physics, 2012, v. 112 n. 1
Issued Date	2012
URL	http://hdl.handle.net/10722/152813
Rights	Creative Commons: Attribution 3.0 Hong Kong License

Effects of internal strain and external pressure on electronic structures and optical transitions of self-assembled $\text{In}_x\text{Ga}_{1-x}\text{As}/\text{GaAs}$ quantum dots: An experimental and theoretical study

Yuan Wen,¹ Mou Yang,² S. J. Xu,^{1,a)} L. Qin,^{3,b)} and Z. X. Shen⁴

¹Department of Physics and HKU-CAS Joint Laboratory on New Materials, The University of Hong Kong, Pokfulam Road, Hong Kong, China

²Laboratory of Quantum Information Technology, School of Physics and Telecommunication Engineering, South China Normal University, Guangzhou 510006, China

³Department of Physics, National University of Singapore, Singapore 117542

⁴School of Physical and Mathematical Sciences, Nanyang Technological University, Singapore 637371

(Received 7 February 2012; accepted 22 May 2012; published online 2 July 2012)

The optical emissive transitions from the ground and excited states of the self-assembled $\text{In}_x\text{Ga}_{1-x}\text{As}/\text{GaAs}$ quantum dots (QDs) at room temperature were experimentally measured as a function of the external hydrostatic pressure by means of the confocal micro-photoluminescence technique. The ground state transition is very weak under zero external pressure and the photoluminescence is dominant by the excited state transition. However, the intensity of the ground state transition monotonically increases with increasing the external pressure and eventually become the dominant transition. Their pressure coefficients (PCs) were determined to be 6.8 and 7.1 meV/kbar, respectively, which were astonishingly smaller than those of GaAs bulk and the $\text{InGaAs}/\text{GaAs}$ reference quantum well. The emission peak from the higher order excited states had a much smaller PC (~ 0.5 meV/kbar). The influence of the built-in strain and external hydrostatic pressure on the electronic structures and optical transitions of various $\text{In}_x\text{Ga}_{1-x}\text{As}/\text{GaAs}$ QDs was theoretically investigated by using the eight-band $\mathbf{k}\cdot\mathbf{p}$ method. Good agreement between the theoretical and experimental results was achieved, firmly revealing that the internal built-in strain in the dot system is mainly responsible for the experimental findings. © 2012 American Institute of Physics. [<http://dx.doi.org/10.1063/1.4730628>]

I. INTRODUCTION

In recent years, there has been considerable interest studying self-assembled $\text{InGaAs}/\text{GaAs}$ quantum dots (QDs) because of their potential applications in novel electronic and optoelectronic devices.^{1–5} It is known that the formation of self-assembled QDs is due to the partial relaxation of the lattice mismatch strain during the heteroepitaxial growth.¹ The residual strain thus exists in and around the QDs, which could have a large impact on the physical and optical properties of the QDs.^{6,7} Photoluminescence (PL) spectroscopy under hydrostatic pressure is an effective tool for exploring electronic structure and optical transition in the QDs. Most of the pressure coefficients (PCs) of the $\text{InGaAs}/\text{GaAs}$ QDs measured by PL under different pressures are about 7.5–9.0 meV/kbar, which is 17%–30% smaller than that found in GaAs bulk.⁸ In 2002, Manjón *et al.* reported that the PC of self-assembled InAs/GaAs QDs was 6.5 meV/kbar.⁹ In 2003, Ma *et al.* observed the photoemissions from both the ground and the first excited states in large InAs/GaAs QDs under high hydrostatic pressure at 15 K, and the PCs of the emissions from the two states were determined to be 6.9 and 7.2 meV/kbar, respectively.¹⁰ However, very few works have been reported

about theoretical analysis of the influence of the hydrostatic pressure on the electronic structures and optical properties in the self-assembled $\text{InGaAs}/\text{GaAs}$ QDs.

In this article, the external hydrostatic pressure influence on the electronic states and optical transitions of the $\text{In}_x\text{Ga}_{1-x}\text{As}/\text{GaAs}$ QDs is investigated experimentally and theoretically. The PCs from the ground and excited states of the self-assembled $\text{InGaAs}/\text{GaAs}$ QDs were measured from the investigation of the room-temperature PL spectra under different hydrostatic pressures and indeed significantly smaller. Based on the eight-band $\mathbf{k}\cdot\mathbf{p}$ method considering piezoelectric effect and strain, electronic states and PCs of $\text{In}_x\text{Ga}_{1-x}\text{As}/\text{GaAs}$ QD are theoretically calculated to explain such small experimental PCs of the QDs. The built-in strain in the InGaAs dot is revealed to accounts for the phenomenon.

II. EXPERIMENTAL

The samples used were InAs/GaAs self-assemble QDs grown on the GaAs substrate with molecular beam epitaxy (MBE). Before the growth of the 1.7 monolayers InAs dot layer and the successive 30 nm GaAs cap layer, a 3 nm $\text{In}_{0.17}\text{Ga}_{0.83}\text{As}$ quantum well (QW) was grown on the same GaAs substrate as the reference QW for the comparison purpose. Other growth details of the sample were described in reference.¹¹ Hydrostatic pressure micro-PL technique was employed to measure the PL spectra of the samples under

^{a)}Author to whom correspondence should be addressed. Electronic mail: sjxu@hku.hk.

^{b)}Present address: STATS ChipPAC Ltd., 5 Yishun Street 23, Singapore 768442.

external hydrostatic pressure. The pressure applied to the sample was provided by a diamond anvil cell. The pressure was calibrated by using the standard ruby-fluorescence technique.¹⁰ The 488.0 nm line of an Ar⁺ ion laser was employed as the excitation light source. The measurements were performed at the room temperature.

From the pressure dependence of PL peaks of the InAs/GaAs QDs, their pressure coefficients were obtained from the linear fitting curves. The PCs of the GaAs bulk substrate and the reference InGaAs/GaAs QW were also determined. Figure 1 shows the micro-PL spectra of the samples under different hydrostatic pressures at the room temperature. PL peaks were resolved and their positions with respect to the external pressure were monitored. At the absence of external pressure, the peaks at 1.417, 1.345, and 1.226 eV were well resolved and were associated to the band-edge transitions of GaAs bulk, InGaAs/GaAs reference QW, and InAs/GaAs QDs, respectively. Their pressure dependences are shown in Fig. 1 by the corresponding dashed-dotted lines. In addition, a shoulder at about 1.130 eV shows a much smaller dependence on the external pressure. Its origin is going to be theoretically discussed in Sec. III. It is also noticed that a weak structure located at the low energy region increases remarkably and eventually becomes the dominant emission as the external pressure increases. Its pressure dependence is also illustrated by the dashed-dotted line in Fig. 1. The identification of these PL peaks and their pressure behaviors certainly require a detailed theoretical work. The energetic positions of the well-resolved PL peaks against the external pressure, and their corresponding least-square linear fitting curves were summarized and depicted in Fig. 2. The PCs of the two main PL peaks of the QDs were found to be 6.8 ± 0.4 and 7.1 ± 0.1 meV/kbar, respectively. The PCs of the reference InGaAs QW and bulk GaAs were determined to be 11.1 ± 0.2 and 11.9 ± 0.4 meV/kbar, respectively. Clearly, the PCs of the QDs are about 40% lower than those of the reference InGaAs QW and the bulk GaAs. As mentioned earlier, one emission peak of the QDs possesses a very small pressure coefficient (0.5 ± 0.3 meV/kbar). These findings are interesting and their explanations are also challenging.

III. THEORETICAL CALCULATIONS

A. Strain, piezoelectric potential, and electronic states of the $\text{In}_x\text{Ga}_{1-x}\text{As}/\text{GaAs}$ QD

It is known that spontaneous growth of the self-assembled InGaAs/GaAs QDs is due to the partial release of strain energy accumulated during the growth. As a result, the residual strain still exists inside the QDs and at their surrounding regions. The valence-force-field (VFF) model with Keating potential^{12–15} was employed to calculate the strain distribution in and around the pyramidal InGaAs/GaAs QD under the hydrostatic pressure. A strain-dependent eight-band $\mathbf{k}\cdot\mathbf{p}$ method considering piezoelectric effect⁶ was used to calculate the electronic structure of the QD.

In the VFF calculations, lattice constant is a key parameter. Considering that the lattice constant of material changes accordingly with the external pressure, the lattice constant of

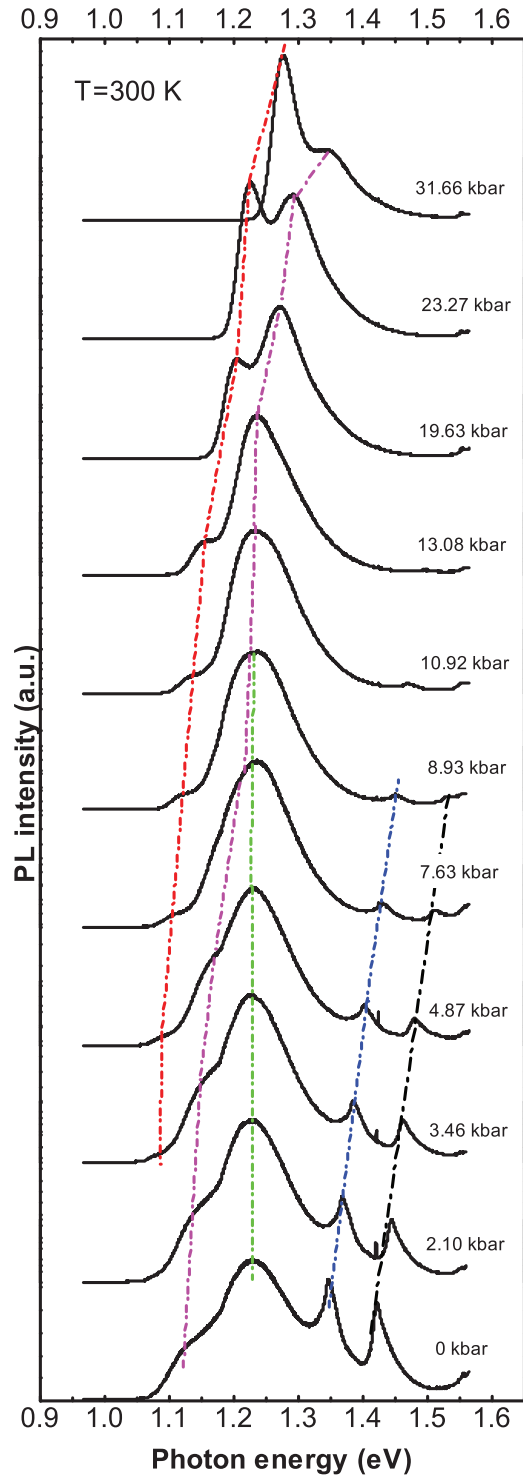


FIG. 1. Measured PL spectra of the InAs/GaAs QDs, InGaAs/GaAs reference QW and GaAs substrate under different hydrostatic pressures at room temperature. The dotted-dashed lines are drawn to guide the eyes for the evolution of the resolved peaks with the external pressure.

the QD system (include the matrix, the wetting layer and the QD) is given as

$$a_{ini}(P) = \left(1 - \frac{P}{C_{11} + 2 \times C_{12}}\right) \times a_0, \quad (1)$$

where P is the hydrostatic pressure, C_{11} and C_{12} are the elastic constants,¹⁶ and a_0 is the lattice constant without

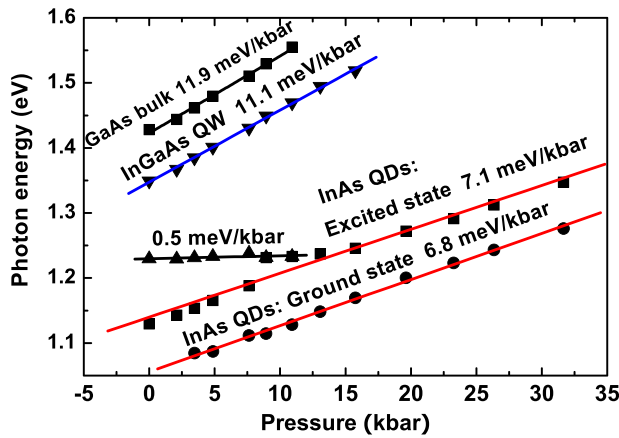


FIG. 2. Experimental PL positions of the InAs/GaAs QDs, InGaAs/GaAs reference QW and GaAs substrate versus the external hydrostatic pressure. Solid lines are the linear fitting curves to the experimental data. The pressure coefficients of various optical transitions can be determined from the fitting.

hydrostatic pressure.⁶ All atomic positions were initiated according to the initial lattice constant and were relaxed to the stable positions by minimizing the total strain energy. After the atomic stable positions were obtained, the strain was calculated. As done in literature, pyramidal structure of QDs was adopted in the calculations. The strain of the pyramidal InAs/GaAs QDs decreased monotonically with the increasing hydrostatic pressure. It implied that the compressive strain of the QD increased but the stretching strain decreased while the external pressure increased.

Due to the existence of the residual strain in the QDs studied here, piezoelectric field may have non-ignorable influence on the electronic structures of the QDs.^{17–19} The piezoelectric charge density is given by

$$\rho_p(\mathbf{r}) = 2\nabla \cdot [\lambda(e_{yz}, e_{zx}, e_{xy})], \quad (2)$$

where λ is the piezoelectric modulus, and e_{ij} is component of the strain tensor. The piezoelectric potential V_p induced by the piezoelectric charge can be calculated from the Poisson equation^{18,19}

$$\rho_p(\mathbf{r}) = \varepsilon_0 \nabla \cdot [\varepsilon(\mathbf{r}) \nabla V_p(\mathbf{r})], \quad (3)$$

where ε_0 and ε are the static dielectric constants of vacuum and the material, respectively. Figure 3 shows the calculated piezoelectric potential at ± 35 meV of the pyramidal InAs/GaAs QD with the base length of 13.6 nm and the height of 6.8 nm. Due to the breakdown of the C_{4v} symmetry of the zinc blende crystal, the piezoelectric potential along the [110] and the $[\bar{1}\bar{1}0]$ directions are opposite, and thus the piezoelectric potential has important impact on the profiles of the electronic states. Figure 4 shows the calculated electron and hole states of the InAs/GaAs QD without ((a) and (b)) and with piezoelectric effect ((c) and (d)), respectively. From the left to right in Figs. 4(a) and 4(c) (4(b) and 4(d)), the wave functions of electron (hole) states E1 (H1), E2 (H2), ..., E6 (H6) are sequentially depicted. Clearly, the piezoelectric field has significant influence on the wave functions of the self-assembled QDs electron and hole states, in

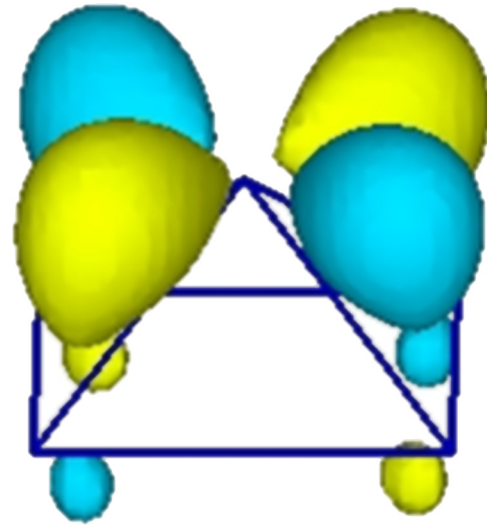


FIG. 3. The isosurfaces of the piezoelectric potentials V_p of the pyramidal InAs/GaAs QD with the base length of 13.6 nm and the height of 6.8 nm, being equal to ± 35 meV (+ green yellow; – light blue).

particular for the excited states with the quantum number of $n \geq 2$. It thus has a large impact on the interband transitions in the self-assembled QDs. It is known that the piezoelectric field is due to the stress induced electric polarization in the crystal lacking of central symmetry. The zinc-blende structure studied in the present work is just one of the simplest cases of such a lattice structure.¹⁸ Therefore, the strength of the resulting piezoelectric field in the self-assembled InGaAs/GaAs QDs is a strong function of both the built-in residual strain and the external pressure. In fact, the piezoelectric field and its effects in self-assembled InAs/GaAs QDs have been addressed by Schliwa *et al.*¹⁸ and Bester *et al.*¹⁹

Figure 5 shows the calculated three-dimensional profiles of the conduction and valance band edges of the InAs/GaAs pyramidal QD. The calculated electron and hole ground states (energetic positions and wave functions) are also depicted as the inset figure. Interestingly, the hole ground state is confined near to the QD bottom more apparently than the electron ground state. As a result, the wave function overlapping of the electron and hole ground states becomes less significant. This could be the main reason leading to the weak PL peaks associated with the electron and hole ground states transitions as observed under the zero external pressure (as shown in Fig. 1).

B. Theoretical PCs of the ground and excited states of the $\text{In}_x\text{Ga}_{1-x}\text{As}/\text{GaAs}$ QDs and the comparison with the experimental data

Considering the possible significant atomic inter-diffusion between the QD and the surrounding barrier material during the growth,²⁰ we calculated the ground and the excited states of the $\text{In}_x\text{Ga}_{1-x}\text{As}/\text{GaAs}$ QDs with different In contents and dot sizes under different hydrostatic pressures. The calculated transition energies (solid symbols) of the ground and the excited states of the InAs/GaAs QD with 6.8 nm in dot height and 13.6 nm in base size (labeled as model 1) and the

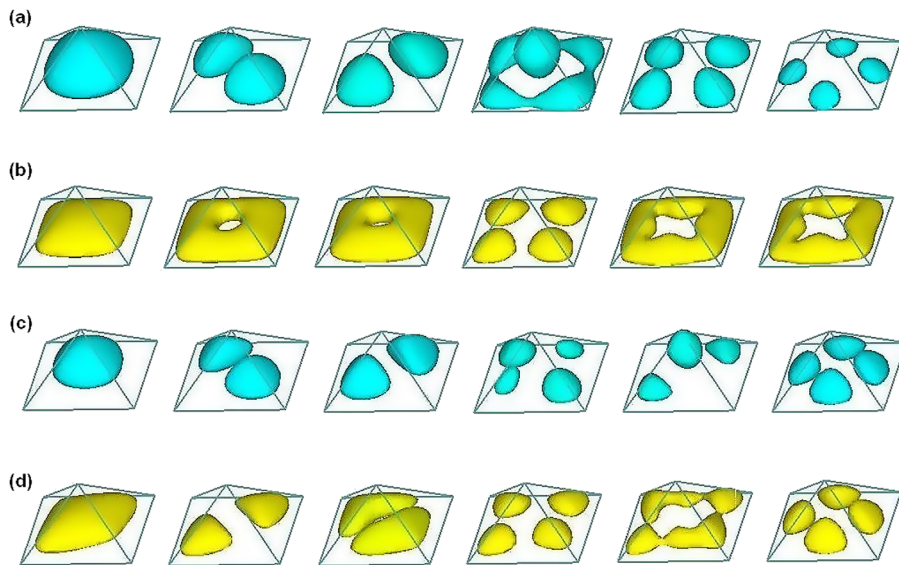


FIG. 4. Calculated electron states and hole states of the pyramidal InAs/GaAs QD with the base length of 13.6 nm and the height of 6.8 nm: (a) Electron states and (b) hole states without piezoelectric effect. (c) Electron states and (d) hole states with piezoelectric effect. From the left to right, the electron (hole) states are E1 (H1), E2 (H2), ..., E6 (H6) in sequence.

$\text{In}_{0.6}\text{Ga}_{0.4}\text{As}/\text{GaAs}$ QD with 4.2 nm in dot height and 8.5 nm in base size (labeled as model 2) are shown in Fig. 6. The calculated results for an $\text{In}_{0.25}\text{Ga}_{0.75}\text{As}/\text{GaAs}$ QW with the well width of 5.7 nm are also shown for comparison. The PCs of the QW and QDs were determined via the linear least-squares fitting, with the fitting curves shown by the solid lines. The theoretical PC of the InGaAs/GaAs QW was found to be 11.2 ± 0.001 meV/kbar, which was in good agreement with the experimental result. The theoretical PCs of the QD model 1 were obtained to be 8.6 ± 0.004 meV/kbar for the ground state and 8.5 ± 0.006 meV/kbar for the excited state, respec-

tively. Those of model 2 were found to be 8.0 ± 0.007 for the ground state and 7.9 ± 0.006 meV/kbar for the excited state. Clearly, the theoretical PCs of the QD model 2 are in better agreement with the experimental data. This indicates that there is significant atomic inter-diffusion between the InAs

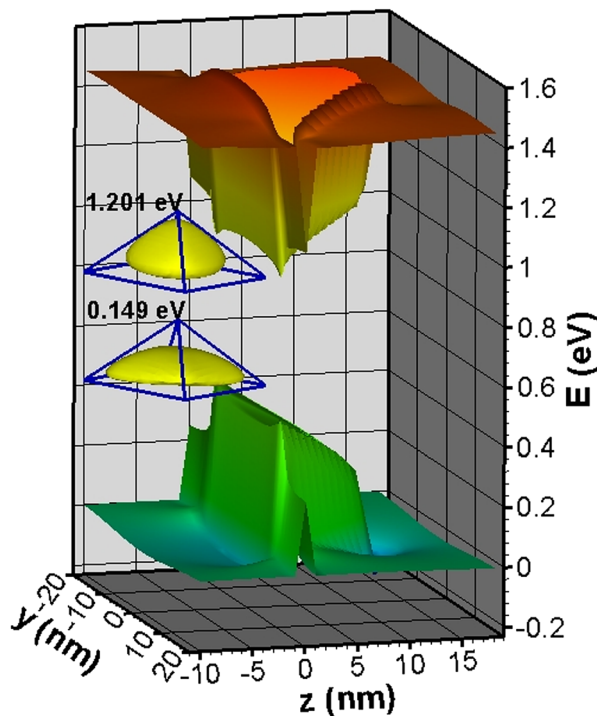


FIG. 5. The calculated three-dimensional band edge potential profiles of the pyramidal InAs/GaAs QD with the same structural parameters as the case shown in Fig. 4. The inset shows the calculated energetic positions and wave functions of electron and hole ground ($n = 1$) states.

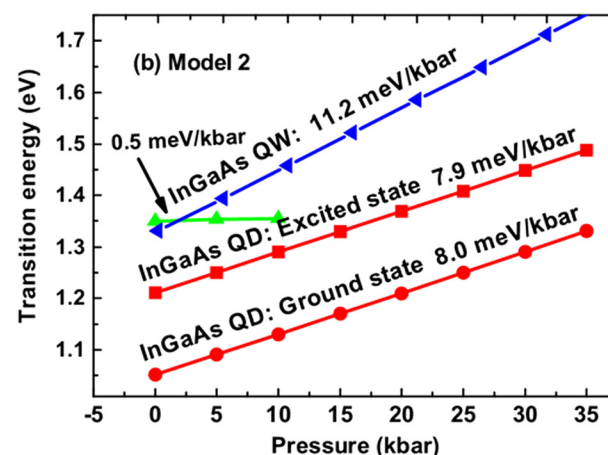
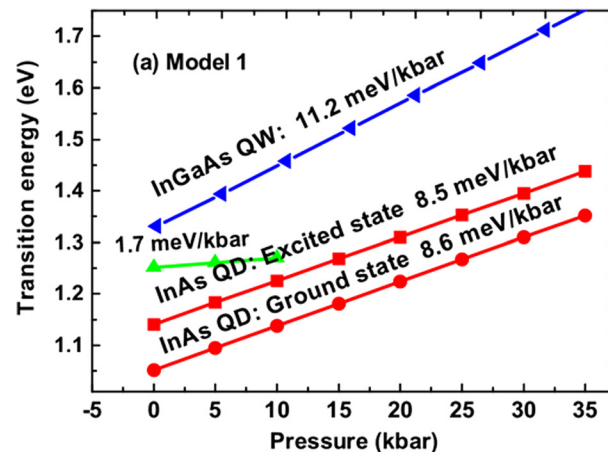


FIG. 6. The calculated transition energies and their PCs of (a) the $\text{In}_{0.6}\text{Ga}_{0.4}\text{As}/\text{GaAs}$ QD, and (b) InAs/GaAs QD. The PC of $\text{In}_{0.25}\text{Ga}_{0.75}\text{As}/\text{GaAs}$ QW with the well width of 5.7 nm is also displayed for comparison.

QDs and the surrounding GaAs. This is consistent with the XRD rocking curve as found in the previous investigation.²⁰ The transition energies from the second and the higher electron excited states to the hole excited states of models 1 and 2 were also calculated. These transitions exhibit much smaller PCs. For example, the PC of the transitions from the second electron excited state to the hole excited state is 0.5 ± 0.2 meV/kbar for the QD model 2. These data give further evidence that model 2 is more appropriate for the self-assembled InAs/GaAs QDs. Interestingly, the band gap values (not shown here) of the $\text{In}_x\text{Ga}_{1-x}\text{As}/\text{GaAs}$ QDs at zero external pressure show an unusual dependence on the In content. They increase with increasing In content, which unambiguously indicates that the built-in strain plays a dominant role in determining the transition energies of the electronic states in the self-assembled InGaAs/GaAs QDs. This is because that the larger In content brings out a larger built-in strain in the dots. Therefore, the built-in strain in the $\text{In}_x\text{Ga}_{1-x}\text{As}/\text{GaAs}$ QD is the main reason why the QD exhibits much smaller PCs. In our previous work on the hydrostatic pressure-dependent PL spectra of $\text{In}_x\text{Ga}_{1-x}\text{N}/\text{In}_y\text{Ga}_{1-y}\text{N}$ QWs,²¹ it has been shown that the large lattice mismatch strain and thus strong piezoelectric field results in a smaller hydrostatic PC of the band-edge optical emissions of the sample. The present work is consistent with this previous observation. In the InGaN/GaN QWs with wurzite structure, there are a large built-in strain and strong piezoelectric polarization effect too.²¹

IV. CONCLUSIONS

The room-temperature PL spectra from the self-assembled InAs/GaAs QDs under different hydrostatic pressures have been measured. The experimental PCs of the transitions from the ground and excited electronic states of the QDs were found to be significantly smaller than those of the InGaAs QW and the GaAs bulk. Moreover, their intensities showed distinctive dependence on the external pressure. The PC of the transition between the higher order excited states was found to be only ~ 0.5 meV/kbar. The theoretical calculations based on the eight-band $\mathbf{k} \cdot \mathbf{p}$ theory and VFF model have been conducted to find the strain profiles and PCs of the transitions in $\text{In}_x\text{Ga}_{1-x}\text{As}/\text{GaAs}$ pyramidal QDs under the different hydrostatic pressures. Good agreement between the experimental and theoretical results was achieved when

appropriate average In content and dot size were adopted. It is thus concluded that the smaller PCs of the QDs are mainly due to the presence of built-in strain in the QDs. Moreover, the calculations showed that the increase of the In content in the dot would lead to the increase of the PCs.

ACKNOWLEDGMENTS

This work was supported by the HK RGC-GRF Grant (No. HKU 7049/08P). One of the authors, S.J.X., wishes to thank Francis C. C. Ling for his critical reading and English editing, C. C. Zheng and X. H. Wang for their assistance in the determination of the fitting errors and preparation of the eps or tif formatted figures, respectively.

- ¹L. Tacak, P. Hawrylak, and A. Wójs, *Quantum Dots* (Springer, Berlin, 1998).
- ²D. Sreenivasan, J. E. M. Haverkort, T. J. Eijkemans, and R. Notzel, *Appl. Phys. Lett.* **90**, 112109 (2007).
- ³N. F. Masse, S. J. Sweeney, I. P. Marko, A. R. Adams, N. Hatori, and M. Sugawara, *Appl. Phys. Lett.* **89**, 191118 (2006).
- ⁴R. B. Laghumavarapu, M. El-Emawy, N. Nuntawong, A. Moscho, L. F. Lester, and D. L. Huffaker, *Appl. Phys. Lett.* **91**, 243115 (2007).
- ⁵J. W. Luo, S. S. Li, J. B. Xia, and L. W. Wang, *Phys. Rev. B* **71**, 245315 (2005).
- ⁶M. Grundmann, O. Stier, and D. Bimberg, *Phys. Rev. B* **52**, 11969 (1995); O. Stier, M. Grundmann, and D. Bimberg, *Phys. Rev. B* **59**, 5688 (1999).
- ⁷C. Pryor, *Phys. Rev. B* **57**, 7190 (1998).
- ⁸S. G. Lyapin, I. E. Itskevich, I. A. Trojan, P. C. Klipstein, A. Polimeni, L. Eaves, P. C. Main, and M. Henini, *Phys. Status Solidi B* **211**, 79 (1999).
- ⁹F. J. Manjón, A. R. Goñi, K. Syassen, F. Heinrichsdorff, and C. Thomsen, *Phys. Status Solidi B* **235**, 496 (2003).
- ¹⁰B. S. Ma, X. D. Wang, F. H. Su, Z. L. Fang, K. Ding, Z. C. Niu, and G. H. Li, *J. Appl. Phys.* **95**, 933 (2004).
- ¹¹S. J. Xu, X. C. Wang, S. J. Chua, C. H. Wang, J. Jiang, W. J. Fan, and X. G. Xie, *Appl. Phys. Lett.* **72**, 3335 (1998).
- ¹²M. Yang, S. J. Xu, and J. Wang, *Appl. Phys. Lett.* **92**, 083112 (2008).
- ¹³P. N. Keating, *Phys. Rev.* **145**, 637 (1966).
- ¹⁴R. M. Martin, *Phys. Rev. B* **1**, 4005 (1970).
- ¹⁵C. Pryor, J. Kim, L. W. Wang, A. J. Williamson, and A. Zunger, *J. Appl. Phys.* **83**, 2548 (1998).
- ¹⁶O. Stier and D. Bimberg, *Phys. Rev. B* **55**, 7726 (1997).
- ¹⁷H. B. Wu, S. J. Xu, and J. Wang, *Phys. Rev. B* **74**, 205329 (2006).
- ¹⁸A. Schliwa, M. Winkelkemper, and D. Bimberg, *Phys. Rev. B* **76**, 205324 (2007).
- ¹⁹G. Bester, A. Zunger, X. Wu, and D. Vanderbilt, *Phys. Rev. B* **74**, 081305R (2006).
- ²⁰S. J. Xu, H. Wang, Q. Li, M. H. Xie, X. C. Wang, W. J. Fan, and S. L. Feng, *Appl. Phys. Lett.* **77**, 2130 (2000).
- ²¹Q. Li, Z. L. Fang, S. J. Xu, G. H. Li, M. H. Xie, S. Y. Tong, X. H. Zhang, W. Liu, and S. J. Chua, *Phys. Status Solidi B* **235**, 427 (2003).